Screening, optimization and characterization of exopolysaccharides produced by novel strains isolated from Moroccan raw donkey milk

Reda Derdak [a], Souraya Sakoui [a], Oana Lelia Pop [b,c,*], Dan Cristian Vodnar [b,d], Boutaina Addoum [a], Abdelhakim Elmakssoudi [e], Faouzi Errachidi [f], Ramona Suharoschi [b,c,*], Abdelaziz Soukri [a], Bouchra El Khalfi [a,*]

[a] Laboratory of Physiopathology, Molecular Genetics & Biotechnology, Faculty of Sciences Aïn Chock, Health and Biotechnology Research Centre, Hassan II University of Casablanca, Maarif B.P 5366, Casablanca, Morocco
[b] Department of Food Science, University of Agricultural Science and Veterinary Medicine, 3-5 Calea Mănăştur, Cluj-Napoca 400372, Romania
[c] Molecular Nutrition and Proteomics Lab, CDS3, Life Science Institute, University of Agricultural Science and Veterinary Medicine, Calea Mănăştur 3-5, Cluj-Napoca 400372, Romania
[d] Food Biotechnology and Molecular Gastronomy, CDS7, Life Science Institute, University of Agricultural Science and Veterinary Medicine, Calea Mănăştur 3-5, Cluj-Napoca 400372, Romania
[e] Department of Chemistry, Laboratory of Organic Synthesis, Extraction, and Valorization, Faculty of Sciences Aïn Chock, Hassan II University of Casablanca, Maarif B.P 5366, Casablanca, Morocco
[f] Laboratory of Functional Ecology and Engineering Environment, Faculty of Sciences and Technologies, Sidi Mohamed Ben Abdellah University, Imouzzer Street, B.P. 2202, Fez, Morocco

ARTICLE INFO

ABSTRACT

Two exopolysaccharides (EPS) producing strains, isolated from raw donkey milk were identified as *Leuconostoc mesenteroides* SL and *Enterococcus viikkiensis* N5 using 16S rDNA sequencing. The Box Benheken design exhibited the highest yield of EPS-SL (672.342 mg/L) produced by SL and of EPS-N5 (901 mg/L) produced by N5. The molecular weight was 1.68×10^4 for EPS-SL and 1.55×10^4 Da for EPS-N5. FTIR, NMR and GC–MS analysis showed that the EPS are heteropolysaccharides. The SEM image showed that the EPS-SL was smooth and represented a lotus leaf shape and EPS-N5 revealed a stiff-like, porous appearance and was more compact than EPS-SL. The TGA analyses showed high thermal stability and degradation temperature. Additionally, the two EPSs possessed antibacterial and antioxidant activity, and the EPS-SL had the stronger antioxidant activity. Consequently, these results suggest that the functional and biological properties of EPS-SL and EPS-N5 imply the potential application in the food and pharmaceutical industries.

Introduction

Because of its persuasive nutrition and functional ingredients, donkey milk has piqued the interest of academics in recent years (Li et al., 2020a). Its chemical composition is very similar to that of human milk due to content in major components as well of minor components (like oligosaccharides)(Derdak et al., 2020). As a result, it has been utilized as an acceptable alternative for babies who have a variety of food allergies and intolerances (Derdak et al., 2020; Vincenzetti et al., 2017). Fermented donkey milk products have recently been presented as essential sources of probiotics and antioxidants with a variety of health advantages. It has increased in popularity as a result of its biological properties, such as antibacterial and antioxidant activity (Vincenzetti et al., 2017). Its antibacterial action resulted from a large microbial variety, primarily lactic acid bacteria (LAB), which are widely regarded as safe microorganisms (GRAS) because of their long and safe usage as starter cultures in fermented foods (Kostelac et al., 2021). LABs are bacilli and cocci-shaped bacteria that form a wide range of microorganisms. The production of lactic acid, which is the end result of the fermentation of various sugars, is a common trait of these bacteria (Derdak et al., 2021; Sakoui et al., 2020). Furthermore, these microorganisms may be a source of antimicrobial and antifungal metabolites

---

* Corresponding authors at: Department of Food Science, University of Agricultural Science and Veterinary Medicine, 3-5 Calea Mănăştur, Cluj-Napoca 400372, Romania (O.L. Pop, R. Suharoschi). Laboratory of Physiopathology, Molecular Genetics & Biotechnology, Faculty of Sciences Aïn Chock, Health and Biotechnology Research Centre, Hassan II University of Casablanca, Maarif B.P 5366, Casablanca, Morocco (B. El khalfi).
E-mail addresses: oana.pop@usamvcluj.ro (O.L. Pop), ramona.suharoschi@usamvcluj.ro (R. Suharoschi), bouchra.elkhalfi@gmail.com (B. El Khalfi).

such as organic acids, reuterin, hydrogenperoxide, diacetyl, carbondioxide, bacteriocins, and exopolysaccharides (EPS), which inhibit pathogens contaminating milk during processing, transport, storage, and preparation (Daba et al., 2021; Kostelac et al., 2021).

EPSs produced by lactic acid bacteria (LAB) are the subject of an increasing number of studies. LABs can produce EPSs that are potentially useful as safe additives to improve texture and viscosity of natural fermented milk products and as stabilizing, emulsifying, and antioxidant agent (Jiang et al., 2021). Moreover, it has been suggested these biopolymers may confer health benefits to the consumer. Some studies have indicated that these EPSs may have immunostimulatory and antitumoral activity (Wu et al., 2021).

These exopolysaccharides are generally composed of repeated units of oligosaccharides. They are divided into two groups: homopolysaccharides and heteropolysaccharides, depending on whether they are made up of one or more types of sugar, and the qualities listed above are all linked to the chemical structure of these substances (Wang et al., 2015a). In consequence, the determination of these carbohydrate linkages is of great importance. Jolly et al. reported that sugar composition, molecular weight, sugar linkages, presence of repeated units and substitutions, affect the biological and technological properties of EPS. Thus, the chemical characterization of novel EPS is crucial for predicting their potential application (Jolly et al., 2002).

To our Knowledge, no study reports the evaluating and characterization of EPSs produced by strains isolated from donkey milk. Therefore, this study was conducted to optimize the production of EPSs from two lactic acid bacteria newly isolated from donkey milk, characterize them and evaluate their antibacterial and antioxidant activity. EPS production was optimized by the Response Surface Methodology (RSM). The characterization of those EPSs was performed using the scanning electron microscopy (SEM), the Fourier transform infrared (FTIR), the Nuclear magnetic resonance (NMR) spectroscopies and the Gas Chromatography Coupled with Mass Spectrometry (GC–MS). Moreover, the thermic stability of the studied EPSs was evaluated by thermogravimetric analysis (TGA) and molecular weight was determined using an U-shaped Ostwald viscometer. Then, the antioxidant and antibacterial activities were also reported.

Materials and methods

Chemicals and reagents

MRS, yeast extract, tryptone, peptone, Mueller-Hinton broth, potassium persulfate were obtained from Biokar diagnostics (Beauvais, France). Sucrose, glucose, lactose, D-glucose, D-xylose, L-arabinose, D-galactose, D-mannose, trichloracetic acid (TCA), potassium bromide (KBr), trifluoroacetic acid, ammonium molybdate, resazurin, pyridine, methanol, ammonium hydroxide, ascorbic acid, acetic anhydride and glacial acetic acid were procured from Sigma-Aldrich (Saint louis, MO, USA). 1,1-diphenyl-2-picrylhydrazyl (DPPH) and 2,2-azinobis-(3-ethylbenzothiazoline-6-sulphonic acid) (ABTS) were purchased from Fluka (Basel, Switzerland). Aluminum chloride (AlCl$_3$), potassium ferricyanide (K$_3$Fe(CN)$_6$), sodium borohydride, phenol and chloroform were obtained from Merck (Darmstadt, Germany).

Sampling and isolation of strains

A sample of donkey's milk was obtained in a sterile tube and transported at 4 °C. The isolation of LAB was carried out on MRS medium agar.

Screening of EPS-producing strains

Isolated strains were screened for EPS-producing phenotype using different methods: i) detection of "ropy" "phenotype (formation of an unbreakable strand when the colony is touched with an inoculation loop)" and "mucoide non-ropy" "phenotype (glistening, smooth and slimy appearance without occurrence of filament) of colonies growing in MRS media and MRS supplemented with 2% of sucrose; ii) viscosity of liquid cultures using" "exopolysaccharide selection medium" " (ESM: 90 g skimmed milk, 3.5 g yeast extract, 3.5 g peptone and 10 g sucrose per litre)".

Molecular identification

A chloroform phenol technique was used to extract DNA, as previously described (Derdak et al., 2021). Total genomic DNA was isolated from samples and utilized as a template for polymerase chain reaction amplification of a 16S ribosomal DNA fragment (PCR). The PCR reactions have been conducted through a DLAB TC1000-G thermocycler. Two pairs of conserved universal primers were used for amplification: Fd1 5′-AGAGTTTGATCCTGGCTCAG-3 'and RP2 5′-ACGGCTACCTTGT-TACGACTT-3′.

The PCR was performed in a total volume of 15 μL composed of approximately 100 ng of genomic DNA, 0.3 μL of each 10 mM dNTP (Promega), 3 μL of 5X buffer (Promega), 0.9 μL of 25 mM MgCl$_2$ (Promega), 0.12 μL of each 10 mM primer and 0.075 μL of Taq polymerase 5U (Promega). The PCR program used was as follow:

95 °C, 2 '/(95 °C, 40′ '- 55 °C, 40′ '- 72 °C, 1′) x35; 72 °C/5 '/4 °C.

The ExoSAP-IT purification kit (GE Healthcare) was used to purify the PCR products, and the BigDye Terminator Kit version 1.0 was used to sequence them (Applied Biosystems). The sequences obtained were corrected using BioEdit, introduced into Geneious prime and aligned via BLAST to determine the degree of similarity of our sequences with those present in the database.

Response surface optimization experiment

Significant factor determination Single-factor

The influence of different parameters was studied by growing the strain in modified (mMRS) or unmodified MRS. For screening carbon source, glucose present in MRS medium was replaced by sucrose or lactose while keeping other components in the medium constant. For screening the nitrogen source, peptone, yeast peptone, or tryptone were used while keeping other components constant. While the inoculum percentage, incubation temperature and incubation time, were constant in all the above conditions, as 1%, 30 °C and 24 h, respectively. The above carbon and nitrogen sources have concentrations of 2%.

For identifying the optimum conditions of inoculum percentage, incubation temperature (30–37 °C) and incubation time (18-48H), unmodified MRS was used. The quantity of total sugar was evaluated using the phenol-sulfuric acid technique (Dubois et al., 1956).

Response surface optimization experiment

Sucrose, peptone, and % inoculum all had a substantial influence on the EPS, according to single-factor screening results. As a result, these three variables were chosen for response surface design (RSM). Design-Expert 11 was used to create the experimental matrix (Table S1).

A Box Behnken design was used to collect experimental data that fits in a complete Quadratic polynomial model describing the response surface across a relatively large range of parameters. Tables S2 and S3 show the range and levels of the experimental variables evaluated. The quadratic equation (Eq. (1)):

$$Y = Y_0 + Y_{1A} + Y_{2B} + Y_{3C} + Y_{4A}^2 + Y_{5B}^2 + Y_{6C}^2 + Y_{7AB} + Y_{8BC} + Y_{9AC}$$

(1)

Where Y is the measured response, A, B and C are the coded independent input variables, Y_0 is the intercept term, Y_1, Y_2, and Y_3 are the coefficients showing the linear effects, Y_4, Y_5 and Y_6, are the quadratic coefficients showing the squared effects and Y_7, Y_8 and Y_9 are the cross-

product coefficients showing the interaction effects. The experiment was repeated 17 times, and the data from the design experiment was utilized to do regression analysis using the program.

Isolation and purification of EPS

The strains were cultivated in MRS medium in optimum conditions found previously. After incubation, the cell-free supernatant was collected by centrifugation at $10000\times$ g for 10 min, and then mixed with 5% trichloroacetic acid (TCA) and kept at 4 °C for 30 min. Centrifugation at $10000\times$ g for 10 min at 4 °C was used to remove the proteins. The supernatant was diluted with two volumes of cold ethanol and kept at 4 °C overnight. The precipitated crude EPS was then recovered using a $10000\times$ g centrifuge at 4 °C for 15 min. The EPS was dissolved in deionized water and dialyzed against deionized water for 48 h at 4 °C using dialysis tube with a MW cut-off of 10 kDa, before being freeze-dried. The crude EPS was fractionated on a Sephadex G-100 column (1.6 cm × 50 cm) and eluted with distilled water at a flow rate of 1 mL/min for further purification. The carbohydrate content of every 4 mL of elution solution was measured using the phenol-sulfuric acid technique (Dubois et al., 1956). The peak fractions were combined, dialyzed, and frozen. For further examination, the pure EPS was employed.

Molecular weight

Different concentrations of samples were produced, and in a U-shaped Ostwald viscometer, the flow time of equal volumes for each concentration at 30 °C was calculated (Gamal et al., 2021). The flow time of the same volume of distilled water was also measured as a control. Thus, specific viscosity/C was computed by converting the relative viscosity value using the formulae below; the specific activity was derived by converting the relative viscosity value using the equations below. (Eqs. (2) and (3)):

$$\eta_r = \frac{t_0\,\eta_0}{t\,\eta} \tag{2}$$

$$\eta_{sp} = \eta_r - 1 = \frac{\eta - \eta_0}{\eta_0} \tag{3}$$

Where η_r is the relative viscosity, and η_{sp} is the specific activity. t_0, t and α_0, α are the time of flux, and the density of samples and solvent, respectively.

The value of the intrinsic viscosity $[\eta]$ was determined by plot $[(\eta-\eta_0)/\eta_0 c)$, where C is the concentration of the sample. It is also defined as the limit of η_{sp}/C when the concentration approach to 0 (Eq. (4)):

$$[\eta] = \lim_{C\to 0}\frac{\eta_{sp}}{C} = \lim_{C\to 0}\frac{\ln\eta_r}{C} \tag{4}$$

The molecular weight was calculated using Mark-Houwink-Sakurada equation (Eq. (5)) (Gamal et al., 2021):

$$Molecular\ weight = 1.42\ \times\ 10^6\ (\eta)^2 \tag{5}$$

Gas Chromatography Coupled with Mass Spectrometry (GC–MS)

The composition of EPS was detected by the method described by Fooladi et al 2019 with slight modifications (Fooladi et al., 2019). 20 mg of EPS was hydrolysed with 1 mL of 2 M trifluoroacetic acid at 100 °C for 2 h. Methanol was added to the sample after hydrolysis and evaporated. The hydrolysate was then converted to alditol acetates using 1 mL sodium borohydride (10% in 1 M ammonium hydroxide) for 1 h at 30 °C. After that, the samples were neutralized with glacial acetic acid and evaporated. 1 mL acetic anhydride and 0.5 mL pyridine were used to acetylate the reduced sugars, which were then incubated at 50 °C for 40 min. The solution was then extracted and evaporated using chloroform. The mixture was reconstituted with 1 mL of methanol before being

analyzed using GC–MS (Shimadzu QP-2010 plus) on a capillary column BP-5 (30 m × 0.25 mm × 0.25 mm).

The monosaccharide was detected using the GC–MS library and validated using the standard monosaccharide (D-glucose, D-xylose, L-arabinose, D-galactose, and D-mannose), which had been derivatized using the same processes as previously indicated.

Fourier-transform infrared spectroscopy (FTIR) and ultra-violet spectral (UV) analysis.

To investigate alternative functionalities, an IRAffinity-1S spectrometer was used to gather FTIR for the EPS-SL and EPS-N5. 2 mg of samples were mixed with 200 mg of KBr to make compressed discs with a diameter of 3 mm, and the spectra was adjusted for KBr background. The pellets were then scanned at a resolution of 4 cm^{-1} and 32 scans in the range of 4000–500 cm^{-1}.

2 mg of samples was dissolved in 1mL of distilled water and analyzed using an UV–visible spectrophotometer, and the spectra were recorded between 190 - 400 nm (Shimadzu UV-1800).

Nuclear magnetic resonance (NMR)

The EPS-SL and EPS-N5 samples were solubilized in deuterium oxide (D2O) and was analyzed. ^{1}H and ^{13}C NMR spectra were registered on a JNM-ECZ500R/S1 FT NMR SYSTEM (JEOL) 500 MHz spectrometer.

Scanning electron microscopy (SEM)

SEM (QUATTRO S-FEG -Thermofisher scientific) was used to examine the surface morphology and microstructure of EPS-SL and EPS-N5 at magnifications of 1000 and 2500. The lyophilized EPS (20 mg) was mounted on a SEM stub, gold sputtered, and analyzed by SEM.

Thermogravimetric analysis

The thermal analysis (TGA) was recorded by a thermogravimetric DTG-60H (SHIMADZU). The EPS-SL and EPS-N5 were placed in an Al$_2$O$_3$ crucible and heated from 10 °C to 600 °C at 10 °C/min. The experiment was performed under a nitrogen atmosphere.

Antioxidant activity

DPPH radical scavenging activity

The DPPH radical scavenging activity of the EPS-SL and EPS-N5 was measured by the Adesulu-Dahunsi method with modifications (Adesulu-Dahunsi et al., 2018). Different concentration of EPS-SL and EPS-N5 (1, 2,3 and 5 mg/mL) was prepared. 1.5 mL of each concentration was mixed with 1.5 mL of DPPH (2.3 mg in 100 mL of methanol).

The mixture was vortexed forcefully and held at room temperature for 30 min before being measured at 517 nm.

The positive standard was ascorbic acid. The experiment was carried out three times.

$$DPPH\ radicals\ scavenging\ activity\ (\%) = \left(\frac{A_b - A_s}{A_s}\right) \times 100 \tag{6}$$

Where A_b is the absorbance of blank and A_s, the absorbance of the sample.

ABTS radical scavenging activity

The ABTS radical scavenging activity was carried out using the Bai technique with minimal changes (Bai et al., 2021). The ABTS radical solution (a combination of 7 mM ABTS and 2.45 mM potassium persulfate) was diluted with PBS to an absorbance of 0.70 ± 0.02 at 734 nm (pH 7.4). 1.5 mL of each EPS sample was combined with 2.5 mL of ABTS radical solution (concentration 1–5 mg/mL). The combination was then

reacted at room temperature for 6 min before being measured at 734 nm. Each experiment was carried out three times in total.

As a positive control, ascorbic acid was employed. The radical scavenging activity of ABTS was determined using the formula (Eq (7)):

$$ABTS\ radicals\ scavenging\ activity\ (\%) = \left(\frac{A_b - A_s}{A_s}\right) \times 100 \qquad (7)$$

Where A_b is the absorbance of blank and A_s, the absorbance of the sample.

Reducing power

The reducing power was calculated in accordance with Amiri et al, with minor modifications (Amiri et al., 2019). Briefly, 1 mL sample at various concentrations was mixed with 0.2 mol/L PBS (2.5 mL) and 1% $K_3[Fe(CN)_6]$ solution (2.5 mL). After incubation at 50 °C for 20 min, 10% TCA (1 mL) was added and centrifuged at 3000× g for 10 min. Then, the upper layer (1 mL) was combined with distilled water (0.6 mL) and 1% $FeCl_3$ (0.4 mL). Finally, the absorbance was determined at 700 nm. Each experiment was carried out three times with ascorbic acid as a positive control.

Phosphomolybdenum assay

The antioxidant activity of EPS-SL and EPS-N5 was evaluated by phosphomolybdenum method (Khan et al., 2012). 1 mL of reagent solution was mixed with an aliquot of each concentration (0.6 M sulphuric acid, 28 mM sodium phosphate and 4 mM ammonium molybdate). The samples were cooled to room temperature and the absorbance was measured at 765 nm after 90 min in a water bath at 95 °C. Each experiment was carried out three times in total.

Antibacterial activity

Bacteria and culture conditions.

Five strains were used for this study, three Gram-positive bacteria; *Staphylococcus aureus*, *Listeria monocytogenes* and *Streptococcus pyogenes*, and two Gram-negative bacteria; *Escherichia coli* and *Salmonella thyphimurium*. All the strains were cultured in Mueller-Hinton and incubated at 37 °C for 24 h.

Determination of minimum inhibitory concentrations (MIC)

Antimicrobial activity was assessed using a modified microdilution approach. A serial dilution procedure was used to determine the MIC using 96 well plates. With wells containing 100 µL of Mueller-Hinton broth, different dilutions of the EPS-SL and EPS-N5 were carried out, and then 10 µL of inoculum was introduced to all of the wells. The microplates were incubated for 24 h at 37°Celsius. After adding 20 µL of resazurin (200 µg/mL) solution to each well and incubating the plates for 2–3 h at 37 °C, the MIC of the samples was determined.

A switch from blue to pink suggests a decrease in resazurin levels and, as a result, bacterial proliferation.

Statistical analysis

Analysis of variance (ANOVA) was used to examine the results, and the Tukey test was used to detect significant differences using GraphPad Prism 7.0 software.

Results and discussion

Screening and identification of EPS-producing strains

10 LABs were isolated from Moroccan raw donkey milk. These LABs were screened on MRS supplemented with sucrose. 8 isolates showed no viscous colonies and 2 isolates showed a viscous and ropy morphology. The 2 LAB isolates were subjected to molecular identification. The 16S

rDNA was used as query sequences to BLAST in Geneious Prime Software, and the sequences with high pairwise identity were selected. The strains were identified as *Leuconostoc mesenteroides* SL and *Enterococcus viikkiensis* N5.

Response surface optimization experiment

Table S1 (Supplementary material) shows the impact of various carbon and nitrogen sources, as well as inoculum variables, on EPS generation by LS and N5. The three carbon sources had a statistically significant difference (p < 0.05), with sucrose (503 and 712 mg/L) being more advantageous for EPS generation by SL and N5, respectively. Our results were consistent with those obtained by Vidhyalakshmi et al. (2016). The findings of the nitrogen source screening revealed that peptone, at levels of 501 and 698 mg/L, was more suitable for the synthesis of EPS by SL and N5. The carbon and nitrogen sources in the culture medium have an impact on EPS generation (Imran et al., 2016).

All those conditions were done with 1% of inoculum, and the change of temperature and incubation time doesn't show any differences in the EPS production. When increasing the percentage of inoculum to 2%, the amount of EPS increased to 495 mg/L. Among the different conditions, the inoculum was proved to be more beneficial, therefore was chosen for further optimization. Verma et al showed that the inoculum influences the production of EPS (Verma & Kumar, 2020). Our results were close to those found by Majumder et al. (2009). Additionally, the ability of N5 to generate EPS was higher than EPS produced by SL.

The RSM studied the effect of 3 variables (Sucrose, peptone and inoculum) on EPS production. Tables S2 and S3 show the Box-Behnken design matrix for EPS generation by SL and N5, respectively, with experimental, actual, and anticipated values. There were 17 experimental runs, each in triplicate, based on the model developed by the program. The equation used to forecast the highest EPS output is shown below after fitting the experimental findings into the Box-Behnken design under the response surface optimization experiment (Eq. (8) and (9)):

$$EPS - SL = +582.61 + 47.32*A - 17.68*B - 8.08*C - 23.4*AB \\ - 32.17*AC + 31*BC \qquad (8)$$

$$EPS - N5 = +861.57 + 53.66*A - 4.38*B - 31.02*C - 2.77*AB - 20*AC \\ - 0.9625*BC - 38.71*A^2 + 9.82*B^2 - 32.35*C^2 \qquad (9)$$

Where A is sucrose, B is peptone and C is inoculum.

The analysis of variance on RSM to optimize EPS production by SL and N5 are shown in Table S4. The results showed that the ANOVA for model 1 (model of EPS produced by SL) and model 2 (model of EPS produced by N5) was significant (p < 0.0001). The significance of Models 1 and 2 was further validated with F-values of 2381.69 and 80.15, respectively.

Model 1 showed that sucrose, peptone and inoculum, and their interactions had statistically significant effects on EPS produced by SL (p < 0.0001). However, model 2 showed sucrose and peptone and their interaction had statistically significant effects on EPS produced by N5 (p < 0.005). Despite this, the concentration of inoculum had no statistically significant influence on EPS production (p < 0.05).

Model 1 had a correlation value of 99.93 % and model 2 had a correlation coefficient of 99.04 %, showing that the regression of the two models was good. Similarly, the corrective decision coefficient (RAdj2) for models 1 and 2 was 99.89 % and 97.8 %, respectively, indicating that most test data variability can be explained by the models. Two independent variables were used to create the three-dimensional response surface graphs, which were used to investigate the ideal level of each variable and its impact on EPS generation.

The latter assists in comprehending the link between each variable's response and experimental levels. These graphs also indicate the
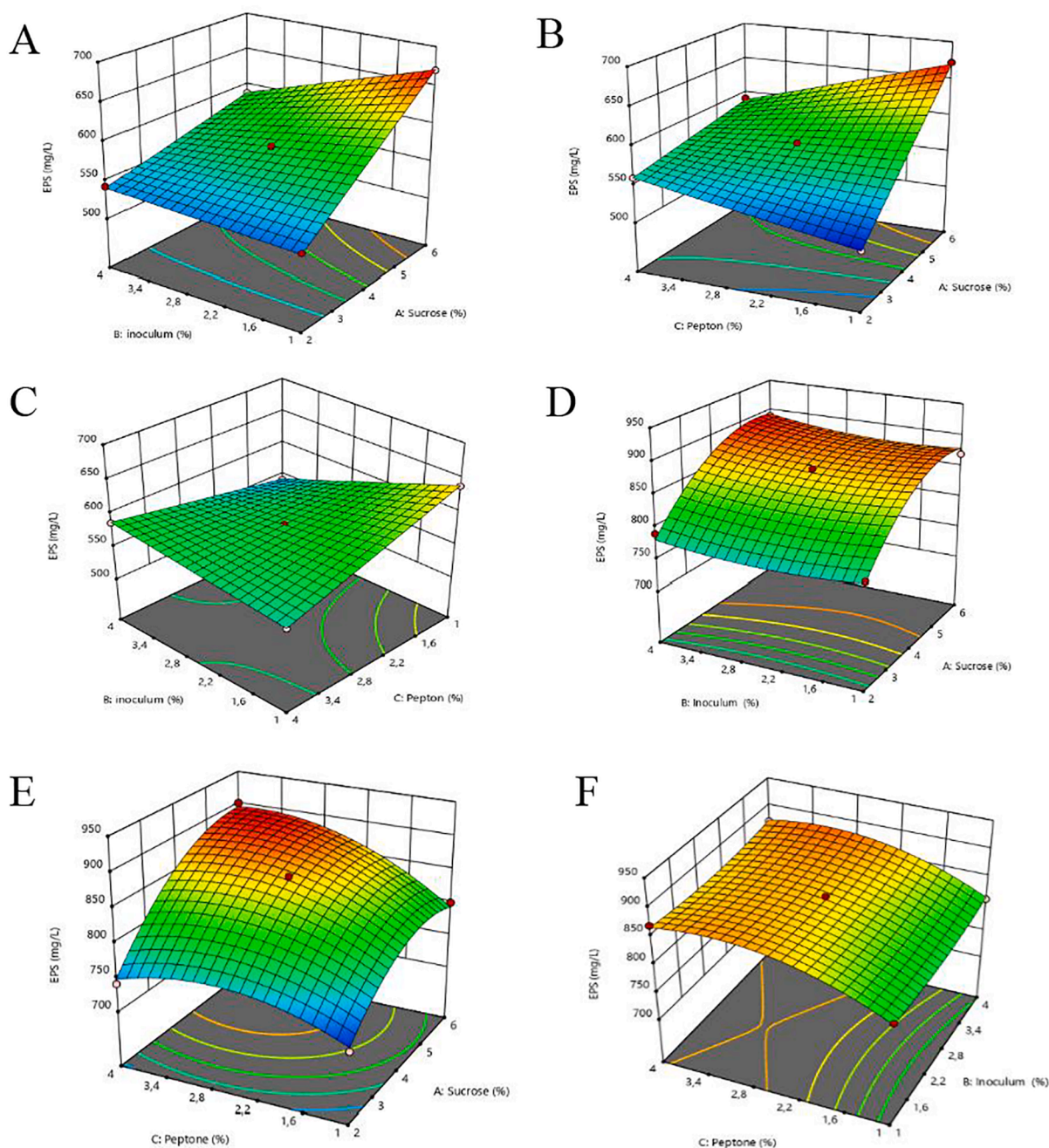
Fig. 1. 3D plot for interactions between independent variables on EPS production by SL (A– C) and N5 (D-F).

interaction between test factors, which aids in determining the best condition (Vidhyalakshmi et al., 2018). By evaluating all feasible combinations, Fig. 1 showed a total of three response surfaces for EPS created by SL and N5, respectively.

The interaction between the tested factors is depicted in these charts, which allows us to find the best condition (Vidhyalakshmi et al., 2016). The maximum amount of EPS-SL (672.34 mg/L) was obtained by a combination of 6% sucrose, 1% inoculum and 2.5% peptone, and for EPS-N5, 901 mg/L was produced by a combination of 6% sucrose, 2.5% inoculum and 4% peptone. While Amiri et al found that the maximum amount of EPS produced by *Bifidobacterium animalis* subsp. lactis BB12 was 160,781 mg/L (Amiri et al., 2019).

According to Fig. 1(A and B), the yield of EPS-SL increased by increasing sucrose and decreasing peptone and inoculum, and there was

a noticeable interaction between inoculum and peptone (Fig. 1C). Furthermore, the yield of EPS-N5 increased by increasing sucrose, peptone and inoculum (Fig. 1D–F).

Purification and molecular weight determination

The crude EPS extracted from SL and N5 was purified by Sephadex G-100 column (Fig. S1; Supplementary material). The results showed a single peak for each EPS, indicating homogeneous polysaccharide. This peak was eluted and freeze-dried. EPS-SL and EPS-N5 have average molecular weights of 1.68×10^4 and 1.55×10^4 Da, respectively. Lactic acid bacteria generate EPS with a molecular weight ranging from 10^4 to 10^6 Da (Daba et al., 2021).

Gas Chromatography Coupled with Mass Spectrometry (GC–MS)

The GC–MS was performed to analyse the monosaccharide composition of EPS-SL and EPS-N5 after alditol acetate derivatization. The results are represented in Fig. 2.

In comparison with standards, the results showed that EPS-SL contained D-glucose (62.84%) and D-galactose (37.16%). However, EPS-N5 was mainly composed of D-glucose (79%), D-galactose (12.7%) and D-mannose (8.3%). These results suggest that the EPS-SL and EPS-N5 were heteropolysaccharides.

The EPS generated by *Leuconostoc mesenteroides XR1* contained glucose and galactose (L. Wang et al., 2021). Li et al presents that the EPS produced by *Leuconostoc mesenteroides SN-8* was composed of glucan and mannose (Li et al., 2020b). The EPS produced by Lactobacillus acidophilus LA5 was composed of glucose (23.25%), mannose (24.49%), galactose (18.46%), and glucuronic acid (19.50%), xylose (8.45%) and fructose (5.85%) (Amiri et al., 2019). Wang et al 2010 showed that EPS produced by *Lactobacillus plantarum KF5* was composed of glucose, mannose and galactose (Y. Wang et al., 2010).

Fourier-transform infrared spectroscopy (FTIR) and ultra-violet spectral (UV) analysis

The UV spectra of the EPS-SL and EPS-N5 revealed no absorption peak at 260 nm or 280 nm, indicating the no existing of aromatic amino acid and nucleic acid (data not shown).

FTIR examination of bacterial EPS revealed a number of peaks that are typical of carbonyl compounds (Fig. 3). The FTIR spectra of the EPS-SL and EPS-N5 samples are presented in the Fig. 3. The two samples (which had comparable spectra) displayed a broad and bright band at roughly 3340 cm^{-1}, which was attributed to the stretching vibration of the carbohydrate hydroxyl groups (Hu et al., 2019), and also a C—H stretching band at around 2930 cm^{-1}. These absorbances represent the polysaccharide fingerprint peak (Amiri et al., 2019). The region of 1655 cm-1 corresponds to the stretching vibration of C = O.

In addition, a band at 1400 is due to C—O, C = O (Cao et al., 2020). Both samples had a specific absorption at 1000–1250 cm^{-1} attributed to the presence of C—O—C glycosidic bonds and C—O—H link bonds of the pyranose unit in each polysaccharide (Ayyash et al., 2020). The absorption peak at 843.59 cm^{-1} was generally formed by α-glycosidic linkages, while the peaks at approximately 915 cm^{-1} were diagnostic of pyranose (Cao et al., 2020). The spectrum showed no significant

difference. Our findings matched those of Cao et al and Vidhyalakshmi et al (Cao et al., 2020; Vidhyalakshmi et al., 2016).

Nuclear magnetic resonance (NMR)

NMR spectroscopy is one of the most often utilized characterization techniques for EPS structural analysis. Fig. 4 shows the ^{1}H and ^{13}C NMR spectra of the EPS-SL and EPS-N5. Generally, the ^{1}H NMR is used to analyze the glycosidic bond configuration of polysaccharides. The proton signal of α-anomeric pyranose is >4.8 ppm, and the proton signal of β-anomeric pyranose is <4.8 ppm (Cao et al., 2020). The anomeric zone (δ 4.5–5.5 ppm), where signals of the anomeric protons of each sugar residue are frequently presented; the ring protons region (δ 3.1–4.5 ppm); and the alkyl groups region, which ranges between δ 1.2–2.3 ppm, make up the ^{1}H NMR spectra of polysaccharides. In the present study, the ^{1}H NMR spectra, two anomeric signal were observed for EPS-SL at δ 4.82 and at δ 4.9, and three signals were observed for EPS-N5 at δ 4.85, δ 4.9 and 5.1. These peaks were characteristics signals of α- (1 → 6) and α- (1 → 3) glycosidic linkage (Bounaix et al., 2009; J. Li et al., 2021). The absorption peak at 4.66 ppm was attributed to D$_2$O.

The ^{13}C NMR spectrum (Fig. 4) of EPS-SL and EPS-N5 included anomeric carbons (95–110 ppm) regions and ring carbons regions (50–85) (Ye et al., 2019). Since the α-pyranose alpha carbon signal is typically δ 97–101 ppm, and the β-pyranose residue is typically δ 101–105 ppm (Cao et al., 2020). Two anomeric carbons regions at δ 97.66 and 97.71 for EPS-SL and 97.78 and 97.85 for EPS-N5 corresponded to α linkage. The other sugar carbon signals appeared between 98 and 65 ppm in the ^{13}C NMR spectrum. A similar kind of ^{13}C NMR interpretation of EPS was reported through signals at 60 to 70 ppm revealed glucose and galactose residues (Wang et al., 2015a). There was no peak at δ >170 ppm, indicating that uronic acid was not present.

Thermogravimetric analysis

The TGA of the EPS-SL and EPS-N5 was done dynamically between weight loss and temperature changes (Fig. S2). The results of the TGA analysis showed three different phases. The EPS-SL and EPS-N5 had an initial weight loss of around 12% from 10 to 150 °C. This immediate decrease of mass might be related to moisture loss. For the EPS-SL no significant mass changes were observed between 150 and 280 °C, which was the highest temperature that EPS-SL can resist. Subsequently, a sharp weight loss (73.5%) was observed from 280 to 340 °C. However,
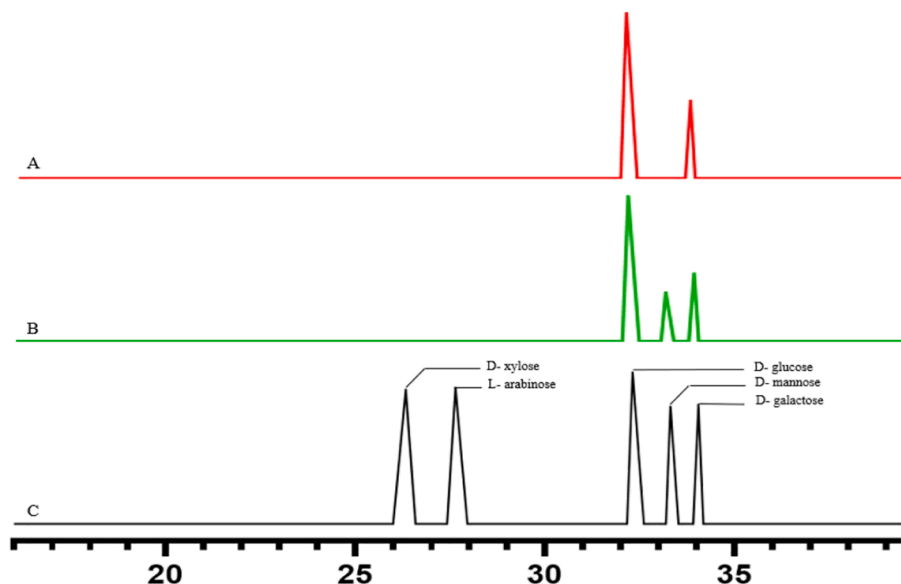
Fig. 2. GC–MS chromatograms of A: EPS-SL, B: EPS-N5 and C: Standards.
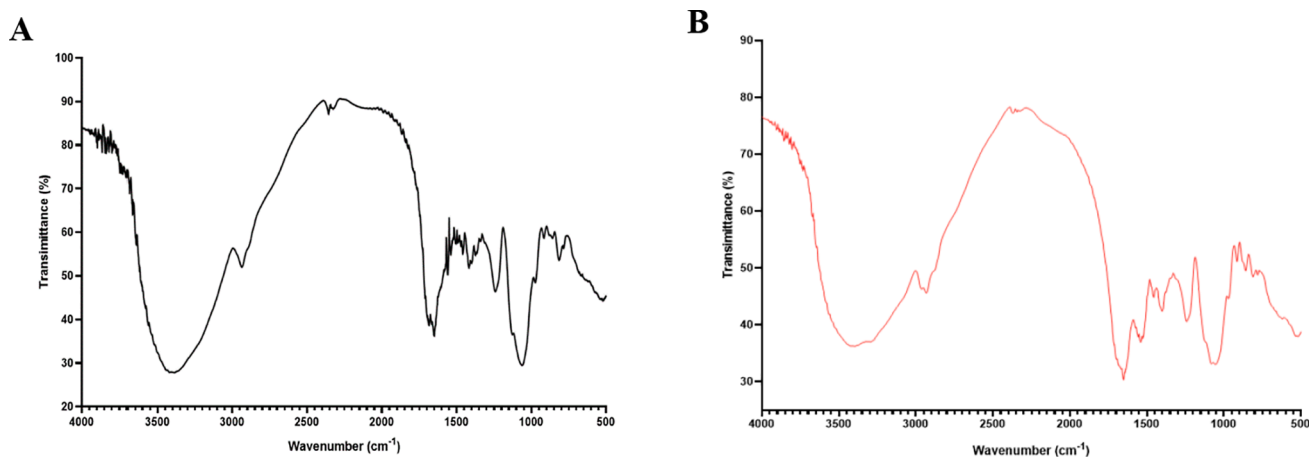
Fig. 3. Fourier-transformed infrared (FT-IR) spectrum of A: EPS-SL and B: EPS-N5.
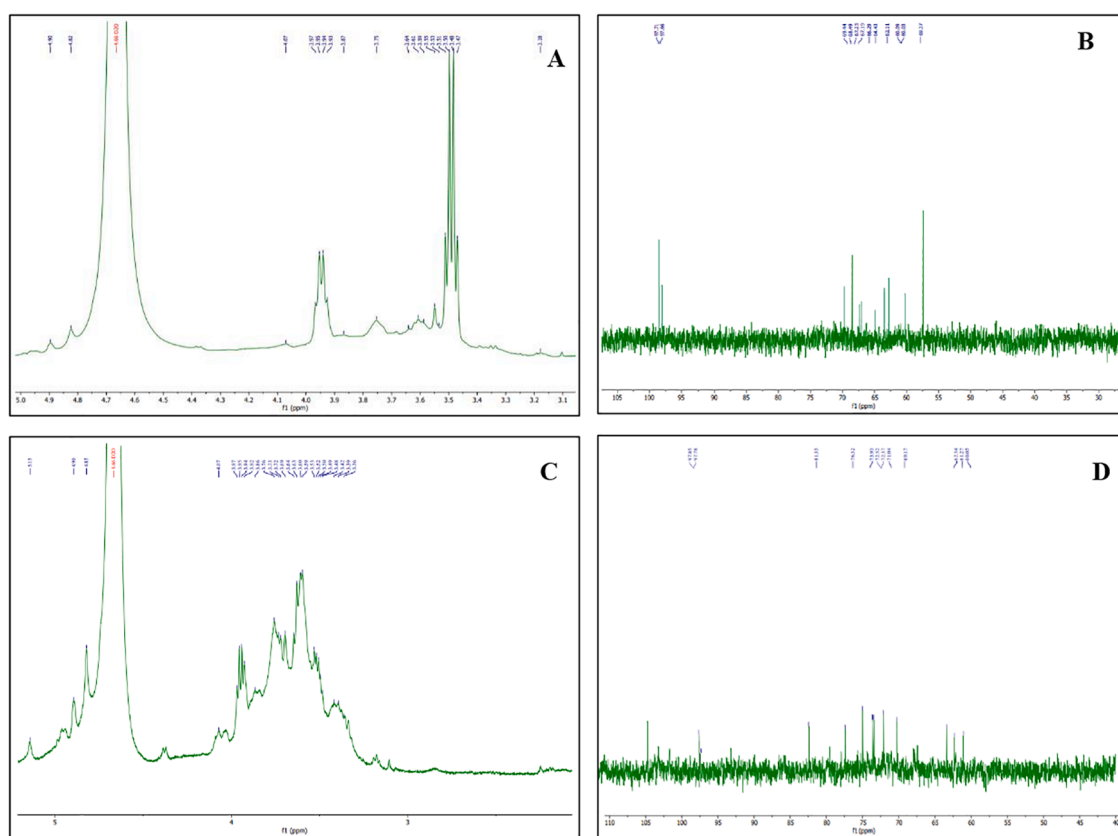
Fig. 4. NMR spectrum of the purified EPS produced by SL: ^{1}H (A) ^{13}C (B) and N5 ^{1}H (C) ^{13}C (D).

for the EPS-N5, a weight loss of 44.8% was observed between 150 and 340 °C.

The EPS mass then steadily dropped, leaving a final residue of 4.5% for EPS-SL and 15.9% for EPS-N5, respectively. Varied carbohydrate compositions are likely to blame for the EPSs' different temperature stability and degradation behavior (Wang et al., 2015b). Thermal stability is a crucial feature to consider for industrial applications of EPS, notably in the food sector, because most food items are manufactured and processed at high temperatures (Bomfim et al., 2020). The thermostable EPS-SL and EPS-N5 are excellent choices for food products.

Scanning electron microscopy (SEM)

The scanning electron microscope (SEM) is a vital instrument for studying the physical properties of polymers, and it may be used to identify the micro-morphology and surface of EPS. The surface structure of EPS-SL and EPS-N5 are shown in Fig. 5. The EPS-SL indicated a three-dimensional architecture with the film surface less compact, richer, and smoother alike a lotus leaf (Fig. 5A and B). L. Wang et al. (2021) conclude that these properties imply the EPS potential of industrial applications for food packaging films and plasticized films. Comparing, the EPS-N5 three-dimensional structure upon increased magnification, revealed a stiff-like, more spherical structure. The EPS feature porous characteristic (Fig. 5C and D). A similar porous structure was also
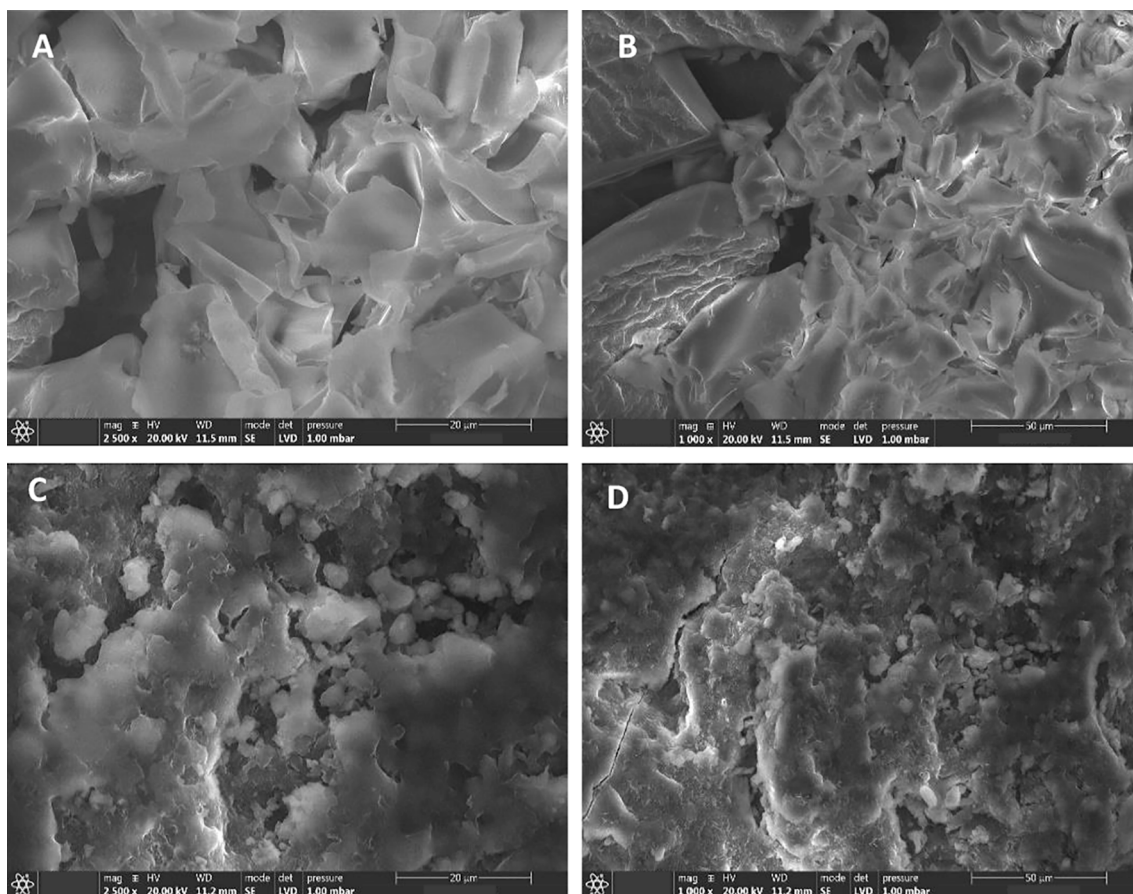
Fig. 5. Scanning electron micro image of EPS-SL (A: 2500×, B: 1000×) and EPS-N5 (C: 2500×, D: 1000×).

reported by the EPS of *Lactobacillus plantarum* YW11 and *Natronotalea sambharensis* sp. nov. (Singh et al., 2019; Wang et al., 2015a). These previous reported studies concluded that because EPS has a more porous and concentrated distribution structure, it may increase its water retention capacity and retain more moisture, thereby expanding the physical properties of the product by generating a hydrated polymer with matrix-like properties and increasing viscosity.
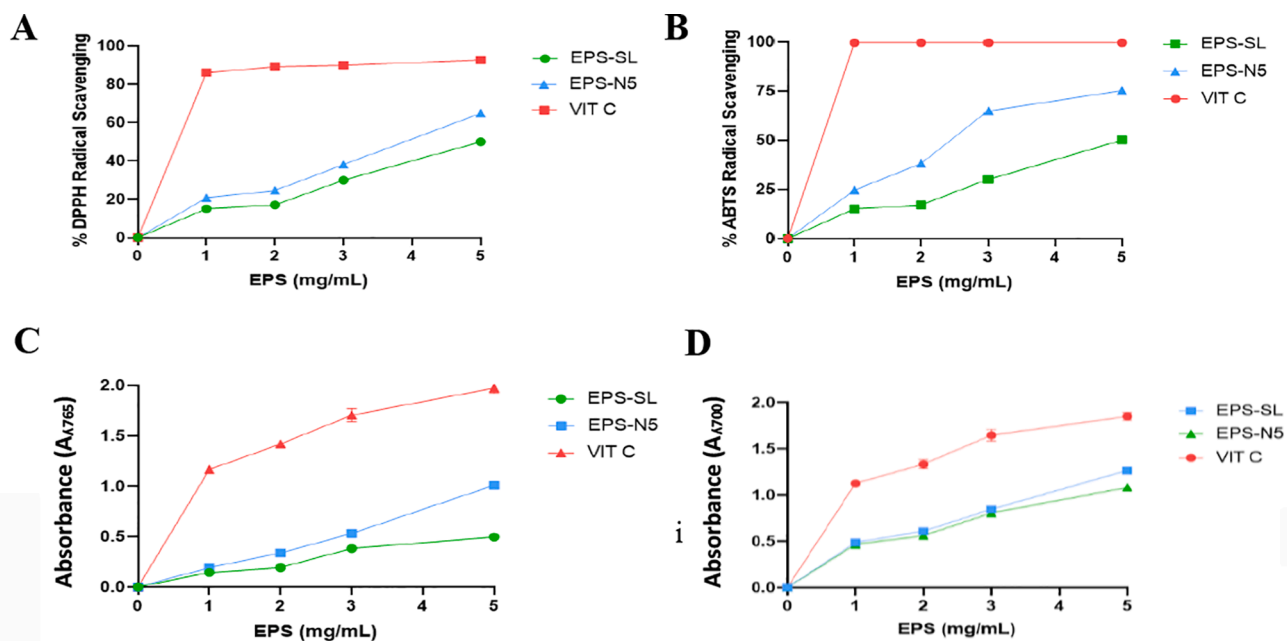
Fig. 6. Antioxidant activity of EPSs with different techniques (A: DPPH, B: ABTS, C: Phosphomolybdenum assay, D: Reducing power).

Biological activity

The EPS-SL and EPS-N5 have bioactivities such as antibacterial and antioxidant activity. The MIC method was used for antibacterial activity and 4 different methods such as DPPH, ABTS, phosphomolybdenum assay and the antioxidant activity of pure EPS-SL and EPS-N5 was investigated using reducing power.

Antioxidant activity

At various doses, the DPPH scavenging activity of EPS-SL and EPS-N5 was tested (Fig. 6A). The scavenging activity of EPS-SL and EPS-N5 increased with increasing concentrations, according to the findings. At 5 mg/mL, EPS-SL and EPS-N5 had maximal DPPH radical scavenging activity of 52.7 and 64.9 %, respectively. Furthermore, the EPS-N5 had a higher scavenging activity than EPS-SL, and both were lower than vit C. At concentrations of 8 and 10 mg/mL, respectively, EPS generated by *Bacillus velezensis* SN −1 and *Lactobacillus plantarum* JLAU103 had the highest DPPH scavenging ability (Cao et al., 2020; Min et al., 2019). This antioxidant capacity of EPS can be attributed to the transfer of hydrogen by the polysaccharide to DPPH while interacting with its radical (Fooladi et al., 2019).

Another method for determining the antioxidant activity of natural items is to utilize the ABTS radical scavenging method. As shown in the Fig. 6B, the scavenging of ABTS radical multiplied with the increase of EPS-SL and EPS-N5 and the maximum clearance was 60.8 and 75.2%, respectively, when the concentration was 5 mg/mL. Ayyash et al observed a lower value than found by our study, with a clearance of 18.49% of EPS produced by *Lactococcus gravieae C47* (Ayyash et al., 2020). Our results were close to those found by Bomfim et al and Xu et al (Bomfim et al., 2020; Xu et al., 2019).

The ABTS radical scavenging activities of EPS-SL and EPS-N5 samples outperformed those of DPPH free radical scavenging. This discrepancy might be explained by the fact that ABTS is a hydrophilic molecule, whereas DPPH is hydrophobic, according to the authors. The reducing power, as an important characteristic of antioxidant activity for natural product. In this assay, the antioxidant agent reduces ferricyanide (Fe^{3+}) to the ferrous (Fe^{2+}) form which was measured at 700 nm. The reducing power of the EPS-SL, EPS-N5 and vit C was shown in Fig. 6D. At 5 mg/mL EPS-SL and EPS-N5 showed a reducing power of 1.08 and 1.26, respectively. Like the other antioxidant test, the reducing power was correlated with its concentrations. In this study, the phosphomolbdenum assay was also studied. This approach is based on antioxidant agents reducing phosphate-molybdenum (VI) to phosphate-molybdenum (V) and forming a green complex at an acidic pH (Choudhuri et al., 2021). The reduction of Mo (VI) increased with the increase of concentration of EPS-SL and EPS-N5, and the maximum reduction was 0.594 and 1.0105, respectively (Fig. 6C).

Antibacterial activity

The antibacterial activity of EPS-SL and EPS-N5 was studied using the minimal inhibitory concentration (MIC) method. The results showed that EPS-SL and EPS-N5 had an interesting antibacterial activity. The MIC of both EPS was 1.75, 2.5 and 5 mg/mL against *S. aureus*, *E. coli* and *L. monocytogenes*, respectively. No effect was observed against *S. pyogenes* and *S. thyphimurium*. In comparison, Ye et al found a MIC of 2 and 3 mg/mL against *E. coli* and *S. aureus* (Ye et al., 2019). Fooladi et al observed no effect against *L. monocytogenes* and found a 3.3 mg/mL MIC against *S. aureus* (Fooladi et al., 2019). The mechanism of antibacterial action may be attributed to the interaction between the EPS and peptidoglycan and disrupt the structure, or the EPS interfere with peptidoglycan synthesis enzyme at substrate level, and stopping the cell wall biosynthesis and disruption. A few studies suggest that the EPS can block channels or receptors on the outer membrane (Abdalla et al., 2021). Another study, report that the EPS facilitate the accumulation of secondary metabolites, which could negatively affect pathogens (Salachna et al., 2018).

Conclusions

In this research, EPS producing strains, isolated from raw donkey milk, was reported as *Leuconosctoc mesenteroides SL* and *Enterococcus vikkiensis N5*. According to the RSM findings, the optimized medium containing sucrose, peptone, and inoculum produced the most EPS. The results of GC–MS, FTIR, and NMR analysis confirmed that the EPS-SL and EPS-N5 are heteropolysaccharides containing various monosaccharide components connected by α-(1 → 6) and -(1 → 3) linkages. The SEM image revealed that the EPS-SL showed a smooth and a lotus leaf shape, and EPS-N5 revealed a stiff-like, porous and more compact than EPS-SL. In addition, EPS-SL and EPS-N5 showed a higher degradation temperature, 280 °C and 340 °C, respectively. Moreover, EPS-SL and EPS-N5 showed an antibacterial activity against *S. aureus, E. coli* and *L. monocytogenes* with a MIC of 1.75, 2.5 and 5 mg/mL, respectively, and also showed an antioxidant activity. Our study suggests that EPS-SL and EPS-N5 may be a potential alternative as a food additive with an important antioxidant and antibacterial activity.

Declaration of Competing Interest

The authors declare that they have no known competing financial interests or personal relationships that could have appeared to influence the work reported in this paper.

Appendix A. Supplementary data

Supplementary data to this article can be found online at https://doi.org/10.1016/j.fochx.2022.100305.

References

Abdalla, A. K., Ayyash, M. M., Olaimat, A. N., Osaili, T. M., Al-Nabulsi, A. A., Shah, N. P., & Holley, R. (2021). Exopolysaccharides as Antimicrobial Agents: Mechanism and Spectrum of Activity. *Frontiers in Microbiology, 12*. https://doi.org/10.3389/FMICB.2021.664395

Adesulu-Dahunsi, A. T., Sanni, A. I., & Jeyaram, K. (2018). Production, characterization and In vitro antioxidant activities of exopolysaccharide from Weissella cibaria GA44. *LWT, 87*, 432–442. https://doi.org/10.1016/J.LWT.2017.09.013

Amiri, S., Rezaei Mokarram, R., Sowti Khiabani, M., Rezazadeh Bari, M., & Alizadeh Khaledabad, M. (2019). Exopolysaccharides production by Lactobacillus acidophilus LA5 and Bifidobacterium animalis subsp. lactis BB12: Optimization of fermentation variables and characterization of structure and bioactivities. *International Journal of Biological Macromolecules, 123*, 752–765. https://doi.org/10.1016/J.IJBIOMAC.2018.11.084

Ayyash, M., Abu-Jdayil, B., Itsaranuwat, P., Almazrouei, N., Galiwango, E., Esposito, G., … Najjar, Z. (2020). Exopolysaccharide produced by the potential probiotic Lactococcus garvieae C47: Structural characteristics, rheological properties, bioactivities and impact on fermented camel milk. *Food Chemistry, 333*, Article 127418. https://doi.org/10.1016/J.FOODCHEM.2020.127418

Bai, Y. P., Zhou, H. M., Zhu, K. R., & Li, Q. (2021). Effect of thermal processing on the molecular, structural, and antioxidant characteristics of highland barley β-glucan. *Carbohydrate Polymers, 271*, Article 118416. https://doi.org/10.1016/J.CARBPOL.2021.118416

Bomfim, V. B., Pereira Lopes Neto, J. H., Leite, K. S., de Andrade Vieira, É., Iacomini, M., Silva, C. M., Olbrich dos Santos, K. M., & Cardarelli, H. R. (2020). Partial characterization and antioxidant activity of exopolysaccharides produced by Lactobacillus plantarum CNPC003. *LWT. 127*. 109349. 10.1016/J.LWT.2020.109349.

Bounaix, M. S., Gabriel, V., Morel, S., Robert, H., Rabier, P., Remaud-Siméon, M., … Fontagné-Faucher, C. (2009). Biodiversity of Exopolysaccharides Produced from Sucrose by Sourdough Lactic Acid Bacteria. *Journal of Agricultural and Food Chemistry, 57*(22), 10889–10897. https://doi.org/10.1021/JF902068T

Cao, C., Li, Y., Wang, C., Zhang, N., Zhu, X., Wu, R., & Wu, J. (2020). Purification, characterization and antitumor activity of an exopolysaccharide produced by Bacillus velezensis SN-1. *International Journal of Biological Macromolecules, 156*, 354–361. https://doi.org/10.1016/J.IJBIOMAC.2020.04.024

Choudhuri, I., Khanra, K., Maity, P., Patra, A., Maity, G. N., Pati, B. R., … Bhattacharyya, N. (2021). Structure and biological properties of exopolysaccharide isolated from Citrobacter freundii. *International Journal of Biological Macromolecules, 168*, 537–549. https://doi.org/10.1016/J.IJBIOMAC.2020.12.063

Daba, G. M., Elnahas, M. O., & Elkhateeb, W. A. (2021). Contributions of exopolysaccharides from lactic acid bacteria as biotechnological tools in food, pharmaceutical, and medical applications. *International Journal of Biological Macromolecules, 173*, 79–89. https://doi.org/10.1016/J.IJBIOMAC.2021.01.110

Derdak, R., Quinteiro, J., Sakoui, S., Addoum, B., Rodríguez Castro, J., Rey Méndez, M., … El Khalfi, B. (2021). Isolation and Identification of Dominant Bacteria from Raw Donkey Milk Produced in a Region of Morocco by QIIME 2 and Evaluation of Their Antibacterial Activity. *Scientific World Journal, 2021*. https://doi.org/10.1155/2021/6664636

Derdak, R., Sakoui, S., Pop, O. L., Muresan, C. I., Vodnar, D. C., Addoum, B., Vulturar, R., Chis, A., Suharoschi, R., Soukri, A., & Khalfi, B. El. (2020). Insights on Health and Food Applications of Equus asinus (Donkey) Milk Bioactive Proteins and Peptides—An Overview. *Foods 2020, Vol. 9, Page 1302, 9*(9), 1302. 10.3390/FOODS9091302.

Dubois, M., Gilles, K. A., Hamilton, J. K., Rebers, P. T., & Smith, F. (1956). Colorimetric method for determination of sugars and related substances. *Analytical Chemistry, 28* (3), 350–356. https://pubs.acs.org/doi/pdf/10.1021/ac60111a017.

Fooladi, T., Soudi, M. R., Alimadadi, N., Savedoroudi, P., & Heravi, M. M. (2019). Bioactive exopolysaccharide from Neopestalotiopsis sp. strain SKE15: Production, characterization and optimization. *International Journal of Biological Macromolecules, 129*, 127–139. https://doi.org/10.1016/J.IJBIOMAC.2019.01.203

Gamal, A. A., Abbas, H. Y., Abdelwahed, N. A. M., Kashef, M. T., Mahmoud, K., Esawy, M. A., & Ramadan, M. A. (2021). Optimization strategy of Bacillus subtilis MT453867 levansucrase and evaluation of levan role in pancreatic cancer treatment. *International Journal of Biological Macromolecules, 182*, 1590–1601. https://doi.org/10.1016/J.IJBIOMAC.2021.05.056

Hu, X., Pang, X., Wang, P. G., & Chen, M. (2019). Isolation and characterization of an antioxidant exopolysaccharide produced by Bacillus sp. S-1 from Sichuan Pickles. *Carbohydrate Polymers, 204*, 9–16. https://doi.org/10.1016/J.CARBPOL.2018.09.069

Imran, M. Y. M., Reehana, N., Jayaraj, K. A., Ahamed, A. A. P., Dhanasekaran, D., Thajuddin, N., … Muralitharan, G. (2016). Statistical optimization of exopolysaccharide production by Lactobacillus plantarum NTMI05 and NTMI20. *International Journal of Biological Macromolecules, 93*, 731–745. https://doi.org/10.1016/J.IJBIOMAC.2016.09.007

Jiang, B., Wang, L., Zhu, M., Wu, S., Wang, X., Li, D., … Tian, B. (2021). Separation, structural characteristics and biological activity of lactic acid bacteria exopolysaccharides separated by aqueous two-phase system. *LWT, 147*, Article 111617. https://doi.org/10.1016/J.LWT.2021.111617

Jolly, L., Vincent, S. J. F., Duboc, P., & Neeser, J.-R. (2002). Exploiting exopolysaccharides from lactic acid bacteria. *Lactic Acid Bacteria: Genetics, Metabolism and Applications, 367*–374. https://doi.org/10.1007/978-94-017-2029-8_26

Khan, R. A., Khan, M. R., Sahreen, S., & Ahmed, M. (2012). Assessment of flavonoids contents and in vitro antioxidant activity of Launaea procumbens. *Chemistry Central Journal, 6*(1). https://doi.org/10.1186/1752-153X-6-43

Kostelac, D., Gerić, M., Gajski, G., Markov, K., Domijan, A. M., Čanak, I., … Frece, J. (2021). Lactic acid bacteria isolated from equid milk and their extracellular metabolites show great probiotic properties and anti-inflammatory potential. *International Dairy Journal, 112*, Article 104828. https://doi.org/10.1016/J.IDAIRYJ.2020.104828

Li, J., Ai, L., Xu, F., Hu, X., Yao, Y., & Wang, L. (2021). Structural characterization of exopolysaccharides from Weissella cibaria NC516.11 in distiller grains and its improvement in gluten-free dough. *International Journal of Biological Macromolecules.*. https://doi.org/10.1016/J.IJBIOMAC.2021.12.089

Li, M., Kang, S., Zheng, Y., Shao, J., Zhao, H., An, Y., … Yang, M. (2020a). Comparative metabolomics analysis of donkey colostrum and mature milk using ultra-high-performance liquid tandem chromatography quadrupole time-of-flight mass spectrometry. *Journal of Dairy Science, 103*(1), 992–1001. https://doi.org/10.3168/JDS.2019-17448

Li, Y., Liu, Y., Cao, C., Zhu, X. Y., Wang, C., Wu, R., & Wu, J. (2020b). Extraction and biological activity of exopolysaccharide produced by Leuconostoc mesenteroides SN-8. *International Journal of Biological Macromolecules, 157*, 36–44. https://doi.org/10.1016/J.IJBIOMAC.2020.04.150

Majumder, A., Singh, A., & Goyal, A. (2009). Application of response surface methodology for glucan production from Leuconostoc dextranicum and its structural characterization. *Carbohydrate Polymers, 75*(1), 150–156. https://doi.org/10.1016/J.CARBPOL.2008.07.014

Min, W. H., Fang, X. B., Wu, T., Fang, L., Liu, C. L., & Wang, J. (2019). Characterization and antioxidant activity of an acidic exopolysaccharide from Lactobacillus plantarum JLAU103. *Journal of Bioscience and Bioengineering, 127*(6), 758–766. https://doi.org/10.1016/J.JBIOSC.2018.12.004

Sakoui, S., Derdak, R., Addoum, B., Serrano-Delgado, A., Soukri, A., & El Khalfi, B. (2020). The Life Hidden Inside Caves: Ecological and Economic Importance of Bat Guano. *International Journal of Ecology, 2020*. https://doi.org/10.1155/2020/9872532

Salachna, P., Mizielińska, M., & Soból, M. (2018). Exopolysaccharide Gellan Gum and Derived Oligo-Gellan Enhance Growth and Antimicrobial Activity in Eucomis Plants. *Polymers, 10*(3), 242. https://doi.org/10.3390/POLYM10030242

Singh, S., Sran, K. S., Pinnaka, A. K., & Roy Choudhury, A. (2019). Purification, characterization and functional properties of exopolysaccharide from a novel halophilic Natronotalea sambharensis sp. nov. *International Journal of Biological Macromolecules, 136*, 547–558. https://doi.org/10.1016/J.IJBIOMAC.2019.06.080

Verma, N., & Kumar, V. (2020). Impact of process parameters and plant polysaccharide hydrolysates in cellulase production by Trichoderma reesei and Neurospora crassa under wheat bran based solid state fermentation. *Biotechnology Reports, 25*, Article e00416. https://doi.org/10.1016/J.BTRE.2019.E00416

Vidhyalakshmi, R., Valli Nachiyar, C., Narendra Kumar, G., & Sunkar, S. (2016). Bacillus circulans exopolysaccharide: Production, characterization and bioactivities. *International Journal of Biological Macromolecules, 87*, 405–414. https://doi.org/10.1016/J.IJBIOMAC.2016.02.001

Vidhyalakshmi, R., Valli Nachiyar, C., Narendra Kumar, G., Sunkar, S., & Badsha, I. (2018). Production, characterization and emulsifying property of exopolysaccharide produced by marine isolate of Pseudomonas fluorescens. *Biocatalysis and Agricultural Biotechnology, 16*, 320–325. https://doi.org/10.1016/J.BCAB.2018.08.023

Vincenzetti, S., Pucciarelli, S., Polzonetti, V., & Polidori, P. (2017). Role of Proteins and of Some Bioactive Peptides on the Nutritional Quality of Donkey Milk and Their Impact on Human Health. *Beverages 2017, Vol. 3, Page 34, 3*(3), 34. 10.3390/BEVERAGES3030034.

Wang, J., Zhao, X., Tian, Z., Yang, Y., & Yang, Z. (2015a). Characterization of an exopolysaccharide produced by Lactobacillus plantarum YW11 isolated from Tibet Kefir. *Carbohydrate Polymers, 125*, 16–25. https://doi.org/10.1016/J.CARBPOL.2015.03.003

Wang, J., Zhao, X., Yang, Y., Zhao, A., & Yang, Z. (2015b). Characterization and bioactivities of an exopolysaccharide produced by Lactobacillus plantarum YW32. *International Journal of Biological Macromolecules, 74*, 119–126. https://doi.org/10.1016/J.IJBIOMAC.2014.12.006

Wang, L., Gu, Y., Zheng, X., Zhang, Y., Deng, K., Wu, T., & Cheng, H. (2021). Analysis of physicochemical properties of exopolysaccharide from Leuconostoc mesenteroides strain XR1 and its application in fermented milk. *LWT, 146*, Article 111449. https://doi.org/10.1016/J.LWT.2021.111449

Wang, Y., Li, C., Liu, P., Ahmed, Z., Xiao, P., & Bai, X. (2010). Physical characterization of exopolysaccharide produced by Lactobacillus plantarum KF5 isolated from Tibet Kefir. *Carbohydrate Polymers, 82*(3), 895–903. https://doi.org/10.1016/J.CARBPOL.2010.06.013

Wu, J., Zhang, Y., Ye, L., & Wang, C. (2021). The anti-cancer effects and mechanisms of lactic acid bacteria exopolysaccharides in vitro: A review. *Carbohydrate Polymers, 253*, Article 117308. https://doi.org/10.1016/J.CARBPOL.2020.117308

Xu, Y., Cui, Y., Wang, X., Yue, F., Shan, Y., Liu, B., … Lü, X. (2019). Purification, characterization and bioactivity of exopolysaccharides produced by Lactobacillus plantarum KX041. *International Journal of Biological Macromolecules, 128*, 480–492. https://doi.org/10.1016/J.IJBIOMAC.2019.01.117

Ye, G., Li, G., Wang, C., Ling, B., Yang, R., & Huang, S. (2019). Extraction and characterization of dextran from Leuconostoc pseudomesenteroides YB-2 isolated from mango juice. *Carbohydrate Polymers, 207*, 218–223. https://doi.org/10.1016/J.CARBPOL.2018.11.092